AD-A127 318 SOUND RADIATION FROM A CYLINDRICAL PIPE COMPOSED OF 1/1
CONCENTRIC LAYERS OF..(U) ADMIRALTY MARINE TECHNOLOGY
ESTABLISHMENT TEDDINGTON (ENGLAND.. E A SKELTON JAN 83
UNCLASSIFIED AMTE(N)/TM83007 DRIC-BR-86949 F/G 13/11 NL

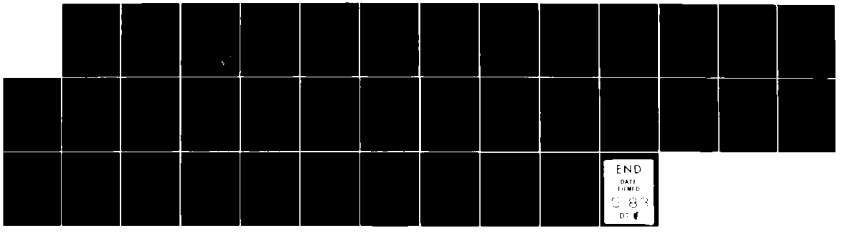

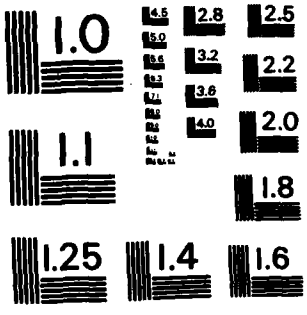

TECH MEMO AMTE(N)TM83007

COPY No 29

ADMIRALTY MARINE TECHNOLOGY ESTABLISHMENT

SOUND RADIATION FROM A CYLINDRICAL PIPE COMPOSED OF CONCENTRIC LAYERS OF FLUIDS AND ELASTIC SOLIDS

E.A.SKELTON

AMTE (Teddington)
Queen's Road TEDDINGTON
Middlesex TW11 0LN

JANUARY 1983

UNCLASSIFIED - UNLIMITED

AMTE(N) TM83007

SOUND RADIATION FROM A CYLINDRICAL PIPE COMPOSED OF CONCENTRIC LAYERS OF FLUIDS AND ELASTIC SOLIDS

BY

E. A. SKELTON

Summary

The cylindrical pipe is composed of a number of concentric layers of elastic solids and fluids. It is excited by time-harmonic mechanical point forces or acoustic sources. The exact linear equations of elasto-dynamics, visco-dynamics and acoustics are solved to obtain, via the finite element method, a matrix equation which connects interface displacements and external forces in the spectral domain. Far-field sound radiation and the wavenumbers of free-waves are obtained from this relation. Numerical results include a comparison of sound radiation levels obtained from the exact theory and a shell theory.

40 pages
11 figures

AMTE(Teddington)
Queen's Road
TEDDINGTON Middlesex TW11 OLN

January 1983

CONTENTS

LIST OF SYMBOLS

(x, y, z)	Cartesian coordinates
(r, φ, z)	cylindrical coordinates
(R, θ, φ)	spherical coordinates
$u_r(r, \varphi, z)$, u_φ, u_z	radial, circumferential and axial displacements
$\bar{u}_r(r, n, \alpha)$, etc.	transforms of displacements
α, n	axial and circumferential harmonic wavenumbers
$\tau_{rr}(r, \varphi, z)$, $\tau_{r\varphi}$, τ_{rz}	stresses within layer
$\bar{\tau}_{rr}(r, n, \alpha)$, etc.	transforms of stresses
$p(r, \varphi, z)$	pressure in fluid
$\bar{p}(r, n, \alpha)$	transform of pressure
p_0	amplitude of point source
F_0	amplitude of point force
$E(\varphi, z)$	external stress
$\bar{E}(n, \alpha)$	transform of external stress
$(r_0, 0, z_0)$	location of point source/force
ω	radian frequency of vibration ($=2\pi f$)
ρ	density
c	sound velocity of acoustic fluid
λ, μ	Lamé constants of elastic layer
μ	dynamic coefficient of viscosity of fluid
k	acoustic wavenumber $= \omega/c$
k_L	longitudinal wavenumber $= \omega(\rho/(\lambda+2\mu))^{1/2}$
k_T	torsional wavenumber $= \omega(\rho/\mu)^{1/2}$
γ	$\sqrt{(k^2-\alpha^2)}$ $\quad \mathrm{Im}(\gamma) \geq 0$
γ_L	$\sqrt{(k_L^2-\alpha^2)}$ $\quad \mathrm{Im}(\gamma_L) \geq 0$
γ_T	$\sqrt{(k_T^2-\alpha^2)}$ $\quad \mathrm{Im}(\gamma_T) \geq 0$

a, b	Inner and outer radii of layer
δ	Dirac delta function
ϵ_n	=1 when n=0, and 2 otherwise
R_0	$=[(r_0^2-2rr_0\cdot\cos(\varphi)+r^2+(z-z_0)^2]^{1/2}$
$J_n, J_n', Y_n, Y_n', H_n, H_n'$	Bessel functions and their derivative $H_n=J_n+iY_n$
$A_1(n,\alpha)$ to $A_6(n,\alpha)$	unknown constants of integration
$[S]_{i*j}$	a matrix, i rows and j columns

$$[\bar{u}(n,\alpha)]_{6*1} = \begin{bmatrix} \bar{u}_r(b,n,\alpha) \\ \bar{u}_\varphi(b,n,\alpha) \\ \bar{u}_z(b,n,\alpha) \\ \bar{u}_r(a,n,\alpha) \\ \bar{u}_\varphi(a,n,\alpha) \\ \bar{u}_z(a,n,\alpha) \end{bmatrix} \qquad [\bar{\tau}(n,\alpha)]_{6*1} = \begin{bmatrix} \bar{\tau}_{rr}(b,n,\alpha) \\ \bar{\tau}_{r\varphi}(b,n,\alpha) \\ \bar{\tau}_{rz}(b,n,\alpha) \\ \bar{\tau}_{rr}(a,n,\alpha) \\ \bar{\tau}_{r\varphi}(a,n,\alpha) \\ \bar{\tau}_{rz}(a,n,\alpha) \end{bmatrix}$$

$$[\bar{u}^i(n,\alpha)]_{3*1} = \begin{bmatrix} \bar{u}_r(b,n,\alpha) \\ \bar{u}_\varphi(b,n,\alpha) \\ \bar{u}_z(b,n,\alpha) \end{bmatrix} \qquad [\bar{\tau}^i(n,\alpha)]_{3*1} = \begin{bmatrix} \bar{\tau}_{rr}(b,n,\alpha) \\ \bar{\tau}_{r\varphi}(b,n,\alpha) \\ \bar{\tau}_{rz}(b,n,\alpha) \end{bmatrix}$$

$$[\bar{u}^e(n,\alpha)]_{3*1} = \begin{bmatrix} \bar{u}_r(a,n,\alpha) \\ \bar{u}_\varphi(a,n,\alpha) \\ \bar{u}_z(a,n,\alpha) \end{bmatrix} \qquad [\bar{\tau}^e(n,\alpha)]_{3*1} = \begin{bmatrix} \bar{\tau}_{rr}(a,n,\alpha) \\ \bar{\tau}_{r\varphi}(a,n,\alpha) \\ \bar{\tau}_{rz}(a,n,\alpha) \end{bmatrix}$$

INTRODUCTION

The mathematical analysis of wave propagation in and sound radiation from a single-layered uniform pipe is usually based on a shell theory to represent the pipe vibrations and the wave equation to represent the interior and exterior acoustic pressures. Recent work using shell theory, of relevance to the problem to be considered here, includes that of Fuller & Fahy [1] who have increased understanding of the physics of wave propagation in fluid-filled pipes through their discussions of wavenumber versus frequency plots and the energy distribution of free-waves between fluid and shell, and that of James [2,3] who has shown that the dispersion relation helps to promote a qualitative understanding of vibration and sound radiation. Only a limited amount of work which uses the exact linear theory of elasticity to represent the vibrations of a fluid-filled pipe has been published; in particular, Lester's derivation [4] of the dispersion relation of thick walled pipes is central to the approach adopted here.

Whilst there is a considerable amount of literature available on wave propagation in and sound radiation by plane layered media, the literature on layered pipes is less extensive. Included in the former is the work of Pestell & James [5] and Spicer [6] who use the exact linear equations of elasto-dynamics, visco-dynamics and acoustics. Included in the latter is the work of Yeh & Chen [7] who study the dynamics of two coaxial shells which are separated by a viscous fluid, and that of Avilova & Rybak [8] who develop the dispersion relation for a thin multi-layered shell.

In this Memorandum, the methods of Lester [4] and Pestell & James [5] are combined to give a matrix relation from which far-field sound radiation and the wavenumbers of free-waves may be calculated numerically by Fortran programs. In addition to being a valuable tool for studying free-wave propagation in and sound radiation from coaxially layered pipes, the programs are useful for studies to determine the range of applicability of shell theories.

2. PROBLEM FORMULATION

(a) General

The layered system shown in Figure 1 is composed of an arbitrary number of concentric elements each of which satisfies the exact linearised equations of acoustics, elasto-dynamics or visco-dynamics. It is excited by time-harmonic point sources which are located in the acoustic fluids, or by time-harmonic point forces applied at the interfaces of the elastic elements. The time factor $\exp(-i\omega t)$ is omitted from all equations.

(b) Fourier Transforms

It is convenient to represent the variables as Fourier transforms. For example, the displacement components are represented by

$$\begin{bmatrix} u_r(r,\varphi,z) \\ u_\varphi(r,\varphi,z) \\ u_z(r,\varphi,z) \end{bmatrix} = (1/2\pi) \sum_{n=0}^{\infty} \begin{bmatrix} \cos(n\varphi) \\ \sin(n\varphi) \\ \cos(n\varphi) \end{bmatrix} \int_{-\infty}^{\infty} \begin{bmatrix} \bar{u}_r(r,n,\alpha) \\ \bar{u}_\varphi(r,n,\alpha) \\ \bar{u}_z(r,n,\alpha) \end{bmatrix} \exp(i\alpha z)\, d\alpha \qquad (2.1)$$

where the spectral displacement components are given by the inverse transform

$$\begin{bmatrix} \bar{u}_r(r,n,\alpha) \\ \bar{u}_\varphi(r,n,\alpha) \\ \bar{u}_z(r,n,\alpha) \end{bmatrix} = (\varepsilon_n/2\pi) \int_{0}^{2\pi} \begin{bmatrix} \cos(n\varphi) \\ \sin(n\varphi) \\ \cos(n\varphi) \end{bmatrix} \int_{-\infty}^{\infty} \begin{bmatrix} u_r(r,\varphi,z) \\ u_\varphi(r,\varphi,z) \\ u_z(r,\varphi,z) \end{bmatrix} \exp(-i\alpha z)\, dz\, d\varphi \qquad (2.2)$$

The Fourier transforms facilitate the solution of linear differential equations by reducing them to algebraic equations.

(c) Construction of the System Matrix Equation

The spectral dynamic stiffness of the layers and the interior and exterior media are matrices which relate spectral stresses to spectral displacements at the interfaces. These matrices

$$[S(n,\alpha)]_{6*6}, \quad [S^e(n,\alpha)]_{3*3} \text{ and } [S^i(n,\alpha)]_{3*3}$$

are obtained for the acoustic, viscous and elastic media in Sections 3-7.

The assembly of the element matrices to form the system dynamic stiffness matrix relation

$$[SM(n,\alpha)]_{M*M}[\bar{U}(n,\alpha)]_{M*1} = [EM(n,\alpha)]_{M*1} \qquad (2.3)$$

is a standard finite element procedure which reflects continuity of displacement and equilibrium of stresses at the interfaces. Computer implementation is straightforward. The matrices $[\bar{U}(n,\alpha)]$ and $[EM(n,\alpha)]$ are column vectors of interface displacements and externally applied interface stresses, respectively, of dimension $M=(3N+3)$ for a system of N layers. The external spectral stresses are defined to be positive when acting in the positive direction of the coordinate axes. With reference to Figures 2 and 3, this sign convention requires changes of sign before assembly to the elements of (i) the last three rows of all matrices $[S(n,\alpha)]$ and (ii) the matrix $[S^e(n,\alpha)]$. An example of an assembled system matrix for a two-layered system is shown in Appendix B.

(d) *Free-Wave Propagation*

In the absence of external forces or sources, the system of homogeneous equations (2.3) has a non-trivial solution if and only if $\det[SM(n,\alpha)]$ vanishes. For given values of n and of ω there will be real and complex values of α at which the determinant vanishes. Real values of α are the wavenumbers at which free-waves propagate. Complex values of α represent evanescent waves, whose amplitudes decrease exponentially with distance.

Here, the real branches only are of interest, and plots of real wavenumber α against frequency for selected circumferential harmonics n are called wavenumber-frequency or dispersion plots.

(e) Far-Field Pressure

In the special case of the exterior medium being an acoustic fluid, the far-field pressure in spherical polar coordinates is found from the stationary phase approximation to be [9]

$$p(R,\theta,\varphi) = -i\omega\rho c \exp(ikR)/\pi R \sum_{n=0}^{\infty} \frac{\bar{U}_1(n,k.\cos\theta)\exp(-in\pi/2)\cos(n\varphi)}{\sin\theta\ H_n'(ka.\sin\theta)} \quad (2.4)$$

where $\bar{U}_1(n,k.\cos\theta)$, the radial spectral displacement of the outermost interface is obtained from the solution of the matrix equation (2.3), evaluated at $\alpha=k.\cos\theta$.

3. THE ACOUSTIC FLUID LAYER

Figure 2 shows a section through an acoustic fluid layer whose inner and outer boundaries, $r=a$ and $r=b$ respectively, are subject to spectral pressures $[\bar{p}(n,\alpha)]$ which produce spectral radial displacements $[\bar{u}_r(n,\alpha)]$.

The pressure in the acoustic fluid layer satisfies the scalar Helmholtz equation

$$\nabla^2 p + k^2 p = 0 \quad (3.1)$$

whose general spectral solution is

$$\bar{p}(r,n,\alpha) = A_1(n,\alpha)J_n(\gamma r) + A_2(n,\alpha)Y_n(\gamma r) \quad (3.2)$$

Evaluation of the pressure and the pressure-displacement relation

$$\partial\bar{p}(r,n,\alpha)/\partial r = \rho\omega^2\bar{u}_r(r,n,\alpha) \quad (3.3)$$

at the boundaries gives the matrix relations

$$\begin{bmatrix} \bar{p}(b,n,\alpha) \\ \bar{p}(a,n,\alpha) \end{bmatrix} = \begin{bmatrix} J_n(\gamma b) & Y_n(\gamma b) \\ J_n(\gamma a) & Y_n(\gamma a) \end{bmatrix} \begin{bmatrix} A_1(n,\alpha) \\ A_2(n,\alpha) \end{bmatrix} \quad (3.4)$$

$$\begin{bmatrix} \bar{u}_r(b,n,\alpha) \\ \bar{u}_r(a,n,\alpha) \end{bmatrix} = \frac{\gamma}{\rho\omega^2} \begin{bmatrix} J_n'(\gamma b) & Y_n'(\gamma b) \\ J_n'(\gamma a) & Y_n'(\gamma a) \end{bmatrix} \begin{bmatrix} A_1(n,\alpha) \\ A_2(n,\alpha) \end{bmatrix} \quad (3.5)$$

from which $[A_1(n,\alpha), A_2(n,\alpha)]^T$ may be eliminated. This gives, after making use of the Wronskian relation

$$J_n(x)Y_n'(x) - J_n'(x)Y_n(x) = 2/\pi x \ ,$$

the matrix relation connecting spectral pressures and displacements at the acoustic fluid layer boundaries as

$$\begin{bmatrix} \bar{p}(b,n,\alpha) \\ \bar{p}(a,n,\alpha) \end{bmatrix} = \frac{\rho\omega^2}{\gamma W} \begin{bmatrix} J_n(\gamma b)Y_n'(\gamma a) - Y_n(\gamma b)J_n'(\gamma a) & -2/\pi\gamma b \\ 2/\pi\gamma a & Y_n(\gamma a)J_n'(\gamma b) - J_n(\gamma a)Y_n'(\gamma b) \end{bmatrix} \begin{bmatrix} \bar{u}_r(b,n,\alpha) \\ \bar{u}_r(a,n,\alpha) \end{bmatrix} \quad (3.6)$$

where

$$W = J_n'(\gamma b)Y_n'(\gamma a) - J_n'(\gamma a)Y_n'(\gamma b)$$

It is convenient when assembling the individual layer matrices into the system matrix to write equation (3.6) in terms of the fluid stresses as

$$\underset{6*6}{[S(n,\alpha)]}\,\underset{6*1}{[\bar{u}(n,\alpha)]} = \underset{6*1}{[\bar{\tau}(n,\alpha)]} \quad (3.7)$$

where the elements of $[S(n,\alpha)]$ are identically zero except for

$$S_{11} = \rho\omega^2(J_n'(\gamma a)Y_n(\gamma b) - J_n(\gamma b)Y_n'(\gamma a))/W$$

$$S_{14} = 2\rho\omega^2/\pi\gamma bW$$

$$S_{41} = -2\rho\omega^2/\pi\gamma aW$$

$$S_{44} = \rho\omega^2(J_n(\gamma a)Y_n'(\gamma b) - J_n'(\gamma b)Y_n(\gamma a))/W$$

4. THE ELASTIC LAYER

Figure 3 shows a section through an elastic layer whose inner and outer boundaries, $r=a$ and $r=b$ respectively, are subject to spectral stresses $[\bar{\tau}(n,\alpha)]$ which produce spectral displacements $[\bar{u}(n,\alpha)]$.

The displacements in the layer satisfy the vector equation of motion [10]

$$(\lambda+\mu)\nabla(\nabla.\underline{u}) + \mu\nabla^2\underline{u} = \rho\partial^2\underline{u}/\partial t^2 \quad (4.1)$$

which may be reduced by using a Lamé substitution

$$\underline{u} = \nabla F + \nabla\wedge\underline{\Psi}, \qquad \underline{\Psi} = (0,0,G) + \nabla\wedge(0,0,H) \quad (4.2)$$

to the three scalar Helmholtz equations

$$\nabla^2F + k_L^2F = 0, \quad \nabla^2G + k_T^2G = 0, \quad \nabla^2H + k_T^2H = 0 \quad (4.3)$$

Lester [4] has shown that the Fourier transform solutions of equations (4.2-4.3) together with the transforms of the stress-displacement relations

$$\begin{aligned} \tau_{rr} &= \lambda(\nabla.\underline{u})+2\mu\partial u_r/\partial r \\ \tau_{r\varphi} &= \mu(\partial u_\varphi/\partial r-(1/r)u_\varphi+(1/r)\partial u_r/\partial\varphi) \\ \tau_{rz} &= \mu(\partial u_r/\partial z+\partial u_z/\partial r) \end{aligned} \tag{4.4}$$

allow the construction of the matrix equation

$$\underset{6*6}{[S(n,\alpha)]}\underset{6*1}{[\bar{u}(n,\alpha)]} = \underset{6*6}{[P(n,\alpha)]}\underset{6*6}{[R(n,\alpha)]^{-1}}\underset{6*1}{[\bar{u}(n,\alpha)]} = \underset{6*1}{[\bar{\tau}(n,\alpha)]} \tag{4.5}$$

connecting spectral displacements and stresses at the boundaries of the elastic layer. The elements of the matrices $[P(n,\alpha)]$ and $[R(n,\alpha)]$ are given in Appendix A.

5. THE VISCOUS FLUID LAYER

Figure 3 is also applicable to a viscous fluid layer whose inner and outer boundaries, r=a and r=b respectively, are subject to spectral stresses $[\bar{\tau}(n,\alpha)]$ which produce spectral displacements $[\bar{u}(n,\alpha)]$.

The linear equations of motion satisfied by the particle velocities and the fluid pressure within the viscous layer [11]

$$\begin{aligned} -\nabla p + \mu\nabla^2\dot{\underline{u}} + (\mu/3)\nabla(\nabla.\dot{\underline{u}}) &= \rho\partial\dot{\underline{u}}/\partial t \\ \partial\rho/\partial t + \rho\nabla.\dot{\underline{u}} &= 0 \\ \partial p/\partial t &= c^2\partial\rho/\partial t \end{aligned} \tag{5.1}$$

may be reduced by means of the substitution

$$\dot{\underline{u}} = \nabla F + \nabla\wedge\underline{\Psi}, \qquad \underline{\Psi} = (0,0,G) + \nabla\wedge(0,0,H) \tag{5.2}$$

to three scalar Helmholtz equations, together with an expression for the fluid pressure, viz.

$$\begin{aligned} \nabla^2F + [\omega^2/(c^2-4k\omega\mu/3\rho)]F &= 0 \\ \nabla^2G + (i\rho\omega/\mu)G &= 0 \\ \nabla^2H + (i\rho\omega/\mu)H &= 0 \end{aligned} \tag{5.3}$$

$$p = -(i\rho/\omega)\nabla.\dot{\underline{u}} \tag{5.4}$$

The stress-velocity relations in the viscous fluid layer are

$$\begin{aligned} \tau_{rr} &= -p-(2\mu/3)\nabla.\dot{\underline{u}} + 2\mu\partial\dot{u}_r/\partial z \\ \tau_{r\varphi} &= \mu(\partial\dot{u}_\varphi/\partial r - (1/r)\dot{u}_\varphi + (1/r)\partial\dot{u}_r/\partial\varphi) \\ \tau_{rz} &= \mu(\partial\dot{u}_r/\partial z + \partial\dot{u}_z/\partial r) \end{aligned} \qquad (5.5)$$

from which, using equation (5.4), p may be eliminated to give the stress-velocity relations for the viscous fluid layer in a form similar to the stress-displacement relations for the elastic layer

$$\begin{aligned} \tau_{rr} &= (ic^2\rho/\omega-2\mu/3)(\nabla.\dot{\underline{u}}) + 2\mu\partial\dot{u}_r/\partial r \\ \tau_{r\varphi} &= \mu(\partial\dot{u}_\varphi/\partial r - (1/r)\dot{u}_\varphi + (1/r)\partial\dot{u}_r/\partial\varphi) \\ \tau_{rz} &= \mu(\partial\dot{u}_r/\partial z + \partial\dot{u}_z/\partial r) \end{aligned} \qquad (5.6)$$

By identifying

$$\begin{aligned} \lambda &= (ic^2\rho/\omega - 2\mu/3) \\ k_T^2 &= i\rho\omega/\mu \\ k_L^2 &= \omega^2/(c^2 - 4i\omega\mu/3\rho) \end{aligned} \qquad (5.7)$$

in equations (5.3) and (5.6) it is evident that the matrix relation between spectral velocities and stresses at the boundaries of the viscous fluid layer is of the same form as that between stresses and displacements at the boundaries of the elastic layer. It is

$$\underset{6*6}{[P(n,\alpha)]}\underset{6*6}{[R(n,\alpha)]^{-1}}\underset{6*1}{[\dot{\bar{u}}(n,\alpha)]} = \underset{6*1}{[\bar{\tau}(n,\alpha)]} \qquad (5.8)$$

or

$$-i\omega\underset{6*6}{[P(n,\alpha)]}\underset{6*6}{[R(n,\alpha)]^{-1}}\underset{6*1}{[\bar{u}(n,\alpha)]} = \underset{6*1}{[\bar{\tau}(n,\alpha)]}$$

where, subject to equations (5.7), the elements of the matrices $[P(n,\alpha)]$ and $[R(n,\alpha)]$ are given in Appendix A.

6. THE INTERIOR MEDIUM

(a) Acoustic Fluid

Figure 2 shows a section through a cylinder of acoustic fluid whose boundary, r=b, is subject to the spectral pressure $\bar{p}(b,n,\alpha)$ which produces the spectral radial displacement $\bar{u}_r(b,n,\alpha)$.

The pressure in the fluid satisfies the scalar Helmholtz equation (3.1), whose general spectral solution equation (3.2) is subject to the condition that the pressure at the origin remains finite, requiring that

$$A_2(n,\alpha) = 0.$$

Evaluation of the pressure equation (3.2) and pressure-displacement relation equation (3.3) at the fluid boundary gives the relations

$$\begin{aligned} \bar{p}(b,n,\alpha) &= A_1(n,\alpha)J_n(\gamma b) \\ \bar{u}_r(b,n,\alpha) &= (\gamma/\rho\omega^2)A_1(n,\alpha)J_n'(\gamma b) \end{aligned} \tag{6.1}$$

from which $A_1(n,\alpha)$ may be eliminated to give the relation connecting spectral pressure and displacement at the boundary

$$\bar{p}(b,n,\alpha) = \rho\omega^2[J_n(\gamma b)/\gamma J_n'(\gamma b)]\bar{u}_r(b,n,\alpha) \tag{6.2}$$

It may be convenient when assembling this element into the system matrix to write equation (6.2) in terms of the fluid stresses as

$$\underset{3*3}{[S^i(n,\alpha)]}\underset{3*1}{[\bar{u}^i(n,\alpha)]} = \underset{3*1}{[\bar{T}^i(n,\alpha)]} \tag{6.3}$$

where the elements of the matrix $[S^i(n,\alpha)]$ are identically zero except for

$$S^i_{11} = -\rho\omega^2 J_n(\gamma b)/\gamma J_n'(\gamma b)$$

(b) Elastic Solid or Viscous Fluid

Figure 3 shows a section through an elastic cylinder whose boundary, r=b, is subject to spectral stress $[\bar{T}^i(n,\alpha)]$ which produces spectral displacement $[\bar{u}^i(n,\alpha)]$.

The displacement in the elastic cylinder satisfies the vector equation of motion (4.1) which may be reduced, by means of the Lamé substitution equation (4.2), to the three Helmholtz equations (4.3) whose spectral solutions, after imposing the requirement that the displacement at the origin remains finite, are

$$\begin{aligned} \bar{F}(r,n,\alpha) &= A_1(n,\alpha)J_n(\gamma_L r) \\ \bar{G}(r,n,\alpha) &= A_2(n,\alpha)J_n(\gamma_T r) \\ \bar{H}(r,n,\alpha) &= A_3(n,\alpha)J_n(\gamma_T r) \end{aligned} \tag{6.4}$$

Evaluation of the displacement equation (4.2) and stress-displacement relations equations (4.4) at the cylinder boundary gives the matrix equations

$$\underset{3*1}{[\bar{u}^i(n,\alpha)]} = \underset{3*3}{[R^i(n,\alpha)]}\begin{bmatrix} A_1(n,\alpha) \\ A_2(n,\alpha) \\ A_3(n,\alpha) \end{bmatrix} \tag{6.5}$$

$$\underset{3*1}{[\bar{T}^i(n,\alpha)]} = \underset{3*3}{[P^i(n,\alpha)]}\begin{bmatrix} A_1(n,\alpha) \\ A_2(n,\alpha) \\ A_3(n,\alpha) \end{bmatrix} \tag{6.6}$$

from which $[A_1(n,\alpha),\ A_2(n,\alpha),\ A_3(n,\alpha)]^T$ may be eliminated. This results in the matrix equation relating spectral stresses and displacements at the cylinder boundary

$$\underset{3*3}{[S^i(n,\alpha)]}\underset{3*1}{[\bar{u}^i(n,\alpha)]} = \underset{3*3}{[P^i(n,\alpha)]}\underset{3*3}{[R^i(n,\alpha)]^{-1}}\underset{3*1}{[\bar{u}^i(n,\alpha)]} = \underset{3*1}{[\bar{\tau}^i(n,\alpha)]} \qquad (6.7)$$

where the elements of the matrices $[P^i(n,\alpha)]$ and $[R^i(n,\alpha)]$ are given in Appendix A.

In the case of a cylinder of viscous fluid, it follows from Section 5 that the matrix equation relating spectral stresses and displacements at the boundary is

$$-i\omega\underset{3*3}{[P^i(n,\alpha)]}\underset{3*3}{[R^i(n,\alpha)]^{-1}}\underset{3*1}{[\bar{u}^i(n,\alpha)]} = \underset{3*1}{[\bar{\tau}^i(n,\alpha)]} \qquad (6.8)$$

where, subject to equations (5.7), the elements of the matrices $[P^i(n,\alpha)]$ and $[R^i(n,\alpha)]$ are given in Appendix A.

7. THE EXTERIOR MEDIUM

(a) Acoustic Fluid

Figure 2 shows a section through the region whose boundary, r=a, is subject to the spectral pressure $\bar{p}(a,n,\alpha)$ which produces the spectral radial displacement $\bar{u}_r(a,n,\alpha)$.

The pressure in the fluid satisfies the scalar Helmholtz equation (3.1), whose general spectral solution equation (3.2) is subject to the radiation condition that at large values of r the pressure consists of outgoing waves only, requiring that

$$A_2(n,\alpha) = iA_1(n,\alpha).$$

Evaluation of the pressure equation (3.2) and pressure displacement relation equation (3.3) at the fluid boundary gives the relations

$$\begin{aligned} \bar{p}(a,n,\alpha) &= A_1(n,\alpha)H_n(\gamma a) \\ \bar{u}_r(a,n,\alpha) &= (\gamma/\rho\omega^2)A_1(n,\alpha)H_n'(\gamma a) \end{aligned} \qquad (7.1)$$

from which $A_1(n,\alpha)$ may be eliminated to give the relation connecting spectral pressure and displacement at the boundary

$$\bar{p}(a,n,\alpha) = \rho\omega^2[H_n(\gamma a)/\gamma H_n'(\gamma a)]\bar{u}_r(a,n,\alpha) \qquad (7.2)$$

It may be convenient when assembling this element into the system matrix to write equation (7.2) in terms of the fluid stresses as

$$[S^{\Theta}(n,\alpha)]_{3*3}[\bar{u}^{\Theta}(n,\alpha)]_{3*1} = [\bar{\tau}^{\Theta}(n,\alpha)]_{3*1} \tag{7.3}$$

where the elements of the matrix $[S^{\Theta}(n,\alpha)]$ are identically zero except for

$$S^{\Theta}_{11} = -\rho\omega^2 H_n(\gamma a)/\gamma H_n'(\gamma a) \tag{7.4}$$

(b) Elastic Solid or Viscous Fluid

The case of an exterior elastic or viscous fluid medium is not relevant to the problem of far-field radiated sound, but it is included for completeness. Figure 3 shows a section through the region whose boundary, r=a, is subject to spectral stress $[\bar{\tau}^{\Theta}(n,\alpha)]$ which produces spectral displacement $[\bar{u}^{\Theta}(n,\alpha)]$.

The displacement in the elastic region satisfies the vector equation of motion (4.1) which may be reduced, by means of the Lamé substitution equation (4.2), to the three Helmholtz equations (4.3) whose spectral solutions after imposing the radiation condition of outgoing waves only are

$$\begin{aligned} \bar{F}(r,n,\alpha) &= A_1(n,\alpha)H_n(\gamma_L r) \\ \bar{G}(r,n,\alpha) &= A_2(n,\alpha)H_n(\gamma_T r) \\ \bar{H}(r,n,\alpha) &= A_3(n,\alpha)H_n(\gamma_T r) \end{aligned} \tag{7.5}$$

Evaluation of the displacement equation (4.2) and stress-displacement relations equations (4.4) at the boundary results, as in Section 6, in the matrix equation relating spectral stresses and displacements at the boundary

$$[S^{\Theta}(n,\alpha)]_{3*3}[\bar{u}^{\Theta}(n,\alpha)]_{3*1} = [P^{\Theta}(n,\alpha)]_{3*3}[R^{\Theta}(n,\alpha)]^{-1}_{3*3}[\bar{u}^{\Theta}(n,\alpha)]_{3*1} = [\bar{\tau}^{\Theta}(n,\alpha)]_{3*1} \tag{7.6}$$

where the elements of the matrices $[P^{\Theta}(n,\alpha)]$ and $[R^{\Theta}(n,\alpha)]$ are given in Appendix A.

In the case of an exterior viscous fluid it follows from Sections 5 and 6 that the matrix relation between spectral stresses and displacements at the boundary is

$$-i\omega[P^{\Theta}(n,\alpha)]_{3*3}[R^{\Theta}(n,\alpha)]^{-1}_{3*3}[\bar{u}^{\Theta}(n,\alpha)]_{3*1} = [\bar{\tau}^{\Theta}(n,\alpha)]_{3*1} \tag{7.7}$$

where, subject to equations (5.7), the elements of the matrices $[P^{\Theta}(n,\alpha)]$ and $[R^{\Theta}(n,\alpha)]$ are given in Appendix A.

8. POINT FORCE EXCITATION

A point force excitation, of magnitude F_0, applied in either the radial or axial direction at cylindrical coordinates $(r_0, 0, z_0)$ on an elastic layer interface may be represented mathematically as the external stress

$$E(\varphi, z) = F_0 \delta(z-z_0)\delta(\varphi)/r_0 \tag{8.1}$$

from which the spectral excitation is obtained via the inverse Fourier transform equation (2.2) as

$$\bar{E}(n, \alpha) = (e_n F_0/2\pi r_0)\exp(-i\alpha z_0) \tag{8.2}$$

The addition of this spectral force into the right-hand-side of the system matrix equation (2.3) is a straightforward finite element procedure.

9. POINT SOURCE IN ACOUSTIC FLUID

(a) Green's Function

The effect of a point source, located at cylindrical coordinates $(r_0, 0, z_0)$ in the acoustic fluid, is best developed via the expansion of its free-space Green's function [12]

$$p_0\exp(ikR_0)/R_0 = (ip_0/2)\sum_{n=0}^{\infty} e_n\cos(n\varphi)\int_{-\infty}^{\infty} J_n(\gamma r_0)H_n(\gamma r)\exp[i\alpha(z-z_0)]d\alpha \qquad r \geq r_0 \tag{9.1}$$

$$= (ip_0/2)\sum_{n=0}^{\infty} e_n\cos(n\varphi)\int_{-\infty}^{\infty} J_n(\gamma r)H_n(\gamma r_0)\exp[i\alpha(z-z_0)]d\alpha \qquad r \leq r_0 \tag{9.2}$$

which is augmented when boundaries are present by a scattering term which satisfies the homogeneous Helmholtz equation (3.1). Thus the total pressure is

$$p(r, \varphi, z) = p_0\exp(ikR_0)/R_0 + p_s(r, \varphi, z) \tag{9.3}$$

where the amplitude of the scattered wave p_s is determined by the boundary conditions.

(b) The Fluid Layer

The spectral form of equation (9.3), representing a source in an acoustic fluid layer, is obtained from equations (9.1), (9.2) and (3.2) as

$$\bar{p}(r,n,\alpha) = (ip_0/2)\epsilon_n J_n(\gamma r_0) H_n(\gamma r) \exp(-i\alpha z_0)$$

$$+ A_1(n,\alpha) J_n(\gamma r) + A_2(n,\alpha) Y_n(\gamma r) \qquad r \geq r_0 \qquad (9.4)$$

$$\bar{p}(r,n,\alpha) = (ip_0/2)\epsilon_n J_n(\gamma r) H_n(\gamma r_0) \exp(-i\alpha z_0)$$

$$+ A_1(n,\alpha) J_n(\gamma r) + A_2(n,\alpha) Y_n(\gamma r) \qquad r \leq r_0 \qquad (9.5)$$

Evaluation of the pressure equation (9.4) or (9.5) and pressure-displacement relation equation (3.3) at the layer boundaries results in the matrix equation relating spectral displacements and stresses at the layer boundaries

$$\underset{6*6}{[S(n,\alpha)]}\,\underset{6*1}{[\bar{u}(n,\alpha)]} = \underset{6*1}{[\bar{\tau}(n,\alpha)]} + \underset{6*1}{[\bar{E}(n,\alpha)]} \qquad (9.6)$$

where the elements of $[\bar{E}(n,\alpha)]$ are identically zero except for

$$\bar{E}_1 = 2ip_0\epsilon_n \exp(-i\alpha z_0)[H_n(\gamma r_0) J_n'(\gamma a) - J_n(\gamma r_0) H_n'(\gamma a)]/W\gamma b$$

$$\bar{E}_4 = 2ip_0\epsilon_n \exp(-i\alpha z_0)[H_n(\gamma r_0) J_n'(\gamma b) - J_n(\gamma r_0) H_n'(\gamma b)]/W\gamma a \qquad (9.7)$$

Equations (9.6) and (9.7) together with the sign convention for external stresses show that the point source in the acoustic fluid layer has an effect on the right-hand-side of the system matrix equation equivalent to external radial spectral stresses of $\bar{E}_1$ and $-\bar{E}_4$ at the upper and lower boundaries respectively.

(c) The Interior Fluid

The spectral form of equation (9.3), representing a source in the interior acoustic fluid, is obtained for the region $r > r_0$ from equations (9.1) and (6.1) as

$$\bar{p}(r,n,\alpha) = (ip_0/2)\epsilon_n J_n(\gamma r_0) H_n(\gamma r) \exp(-i\alpha z_0) + A_1(n,\alpha) J_n(\gamma r) \qquad (9.8)$$

Evaluation of the pressure and pressure-displacement relation, as in Section 6, results in the matrix equation relating spectral displacements and stresses at the boundary as

$$\underset{3*3}{[S^i(n,\alpha)]}\,\underset{3*1}{[\bar{u}^i(n,\alpha)]} = \underset{3*1}{[\bar{\tau}^i(n,\alpha)]} + \underset{3*1}{[\bar{E}^i(n,\alpha)]} \qquad (9.9)$$

where the elements of $[\bar{E}^i(n,\alpha)]$ are identically zero except for

$$E_1^i = 2p_0\epsilon_n \exp(-i\alpha z_0) J_n(\gamma r_0)/\gamma b J_n'(\gamma b) \qquad (9.10)$$

Equations (9.9) and (9.10) show that the point source in the interior acoustic fluid has an effect on the right-hand-side of the system matrix equation equivalent to the external radial spectral stress $\bar{E}_1^i$ at the boundary.

(d) The Exterior Fluid

The spectral form of equation (9.3), representing a source in the exterior acoustic fluid, is obtained for the region $r<r_0$ from equations (9.2) and (7.1) as

$$\bar{p}(r,n,\alpha) = (ip_0/2)\epsilon_n J_n(\gamma r) H_n(\gamma r_0)\exp(-i\alpha z_0) + A_1(n,\alpha) H_n(\gamma r) \qquad (9.11)$$

Evaluation of the pressure and pressure-displacement relation, as in Section 7, results in the matrix equation relating spectral displacements and stresses at the boundary as

$$\underset{3*3}{[S^e(n,\alpha)]}\,\underset{3*1}{[\bar{u}^e(n,\alpha)]} = \underset{3*1}{[\bar{T}^e(n,\alpha)]} + \underset{3*1}{[\bar{E}^e(n,\alpha)]} \qquad (9.12)$$

where the elements of $[\bar{E}^e(n,\alpha)]$ are identically zero except for

$$\bar{E}_1^e = -2p_0\epsilon_n\exp(-i\alpha z_0) H_n(\gamma r_0)/\gamma a H_n'(\gamma a) \qquad (9.13)$$

Equations (9.12) and (9.13) show that the point source in the exterior acoustic fluid has an effect on the right-hand-side of the system matrix equation equivalent to external spectral radial stress of $-\bar{E}_1^e$ at the boundary.

10. NUMERICAL RESULTS

(a) General

Fortran programs have been written to calculate and plot the axial wavenumbers of free-vibration and the far-field sound level due to point source or point force excitation. The programs are written in double precision complex arithmetic which is simulated [6] by the use of double precision variables of leading dimension 2. They were run on a PDP-11/34A computer for which the arithmetic word length of 32 bits used for single precision complex arithmetic is inadequate in this type of problem.

The material and geometric constants in SI units which are used in the calculations, involving a single pipe and two coaxial pipes separated by water, are as follows:

Steel Inner Pipe: $\lambda=10.44\times10^{10}$ $\mu=7.56\times10^{10}$ $\rho=7700.0$
$a=0.2096$ $b=0.2350$

Steel Outer Pipe: $\lambda=10.44\times10^{10}$ $\mu=7.56\times10^{10}$ $\rho=7700.0$
$a=0.2700$ $b=0.3000$

Water: $\rho=1000.0$ $c=1500.0$

Air: $\rho=1.21$ $c=343.0$

Damping in the pipe walls is included by setting λ and μ to the complex

values $\lambda(1-i\eta_\lambda)$ and $\mu(1-i\eta_\mu)$, respectively, where the numerical values of the hysteretic loss factors, η_λ and η_μ, are chosen as 0.02.

(b) Wavenumber Plots

Figure 4 shows the real branches of the wavenumber versus frequency plots, for the first three circumferential harmonics, of the inner pipe containing water and surrounded by a vacuum. The plots are identical to those obtained by Lester [4] who has also superimposed plots obtained from a shell theory. The physical interpretation of the plots is given elsewhere [1].

Figure 5 shows the plots for the composite pipe consisting of the inner and outer pipes separated by a 3.50cm layer of water: again the interior is water and the exterior a vacuum. The plots contain many more branches than the previous plots because of the partial independence of waves in the solids and fluids.

(c) Sound Radiation Spectra

Figures 6-11 show the variation of far-field 'airborne' sound pressures (dB ref. 1 micropascal at 1m) with frequency. The plots (all at φ=0°) consist of straight line joins which connect levels computed at 15Hz spacing: hence, the sharp peaks are unlikely to have been resolved fully. The excitation is either a 1N rms radial force applied to the inner pipe at the cylindrical coordinates (0.2096,0,0), or it is an interior point source, located at (0.1482,0,0), whose free-field pressure is 120dB.

(d) Radiation from Inner Pipe

Figure 6a shows the airborne sound radiation from the inner pipe at θ=90° due to point force excitation. Figures 7a, 8a and 9a show the sound radiation, at θ=90°, 80° and 70°, respectively, due to point-source excitation. The corresponding (b) Figures contain the sound radiation calculated from a shell theory. There is good agreement between the (a) and (b) spectra up to the 'ring frequency' of 3.6kHz, the differences thereafter being mainly attributable to the relatively increasing density of the peaks in shell theory.

James [2] has demonstrated, using shell theory, that the frequencies at which 'peaks' appear in the sound spectra depend on the location (θ) of the observation point. These frequencies are the frequencies at which the lines α=k.cos(θ) cross the wavenumber branches, where k is the wavenumber in air. The same is true when exact linear theory is used. In fact, the difference between the (a) and (b) plots is reflected in the differences between the dispersion plots of the shell and exact theories.

(e) Radiation from Composite Pipe

Figure 10 shows the airborne sound radiated at $\theta=90°$ for the cases of (a) point force excitation: and (b) point source excitation. Figure 11 shows the sound radiation due to point-source excitation calculated at (a) $\theta=80°$ and (b) $\theta=70°$.

Again, the frequency at which 'peaks' appear in the spectra may be found from the dispersion plots as the frequencies at which the lines $\alpha=k.\cos(\theta)$ cross the wavenumber branches. The dispersion relation is equally useful in interpreting the spectra from layered pipes.

E A Skelton (SO)

REFERENCES

1. FULLER., C.R., FAHY, F.J., Characteristics of Wave Propagation and Energy Distribution in Cylindrical Elastic Shells Filled with Fluid, J. Sound and Vib., 81(4), 1982, pages 501-508.

2. JAMES, J.H., Sound Radiation From Fluid Filled Pipes, Admiralty Marine Technology Establishment, Teddington, AMTE(N)TM81048, September 1981.

3. JAMES, J.H., Computation of Acoustic Power, Vibration Response and Acoustic Pressures of Fluid-filled Pipes, Admiralty Marine Technology Establishment, Teddington, AMTE(N)TM82036, May 1982.

4. LESTER, S.A., Free-Wave Propagation in Fluid-Loaded Thick-Walled Circular Pipes, Admiralty Marine Technology Establishment, Teddington, AMTE(N)TM81093, November 1981.

5. PESTELL, J.L., JAMES, J.H., Sound Radiation From Layered Media, Admiralty Marine Technology Establishment, Teddington, AMTE(N)TM79423, October 1981.

6. SPICER, W.J., Free-Wave Propagation in and Sound Radiation by Layered Media with Flow, Admiralty Marine Technology Establishment, Teddington, AMTE(N)TM82102, December 1982.

7. YEH, T.T., CHEN, S.S., Dynamics of a Cylindrical Shell System Coupled by Viscous Fluid, J. Acoust. Soc. Am., 62(2), August 1977, pages 262-270.

8. AVILOVA, G.M., RYBAK, S.A., Normal Modes in Layered Cylindrical Shells, Sov. Phys. Acoust., 25(1), January-February 1979, pages 10-12.

9. JUNGER, M.C., FEIT, D., Sound Structures and their Interaction, MIT Press, 1972.

10. ACHENBACH, J.D., Wave Propagation in Elastic Solids, North Holland/ American Elsevier, 1973.

11. HUNTER, S.C., Mechanics of Continuous Media, Ellis Horwood, 1976.

12. SKELTON, E.A., Free-Space Green's Functions of the Reduced Wave Equation, Admiralty Marine Technology Establishment, Teddington, AMTE(N)TM82073, September 1982

APPENDIX A

The Elastic Layer Matrices $[P(n,\alpha)]_{6\times6}$ and $[R(n,\alpha)]_{6\times6}$

$$P_{11} = 2\mu\gamma_L^2 J_n''(\gamma_L b) - \lambda k_L^2 J_n(\gamma_L b)$$

$$P_{12} = 2\mu\gamma_L^2 Y_n''(\gamma_L b) - \lambda k_L^2 Y_n(\gamma_L b)$$

$$P_{13} = (2\mu n/b^2)[\gamma_T b J_n'(\gamma_T b) - J_n(\gamma_T b)]$$

$$P_{14} = (2\mu n/b^2)[\gamma_T b Y_n'(\gamma_T b) - Y_n(\gamma_T b)]$$

$$P_{15} = -2i\alpha\mu\gamma_T^2 J_n''(\gamma_T b)$$

$$P_{16} = -2i\alpha\mu\gamma_T^2 Y_n''(\gamma_T b)$$

$$P_{21} = (2n\mu/b^2)[J_n(\gamma_L b) - \gamma_L b J_n'(\gamma_L b)]$$

$$P_{22} = (2n\mu/b^2)[Y_n(\gamma_L b) - \gamma_L b Y_n'(\gamma_L b)]$$

$$P_{23} = (\mu/b^2)[2\gamma_T b J_n'(\gamma_T b) + (\gamma_T^2 b^2 - 2n^2) J_n(\gamma_T b)]$$

$$P_{24} = (\mu/b^2)[2\gamma_T b Y_n'(\gamma_T b) + (\gamma_T^2 b^2 - 2n^2) Y_n(\gamma_T b)]$$

$$P_{25} = (2i\alpha\mu n/b^2)[b\gamma_T J_n'(\gamma_T b) - J_n(\gamma_T b)]$$

$$P_{26} = (2i\alpha\mu n/b^2)[b\gamma_T Y_n'(\gamma_T b) - Y_n(\gamma_T b)]$$

$$P_{31} = 2i\alpha\mu\gamma_L J_n'(\gamma_L b)$$

$$P_{32} = 2i\alpha\mu\gamma_L Y_n'(\gamma_L b)$$

$$P_{33} = (i\alpha n\mu/b) J_n(\gamma_T b)$$

$$P_{34} = (i\alpha n\mu/b) Y_n(\gamma_T b)$$

$$P_{35} = \mu\gamma_T(2\alpha^2 - k_T^2) J_n'(\gamma_T b)$$

$$P_{36} = \mu\gamma_T(2\alpha^2 - k_T^2) Y_n'(\gamma_T b)$$

Rows 4, 5, and 6 are obtained by setting b=a in rows 1, 2, and 3.

$$R_{11} = \gamma_L J_n'(\gamma_L b)$$

$$R_{12} = \gamma_L Y_n'(\gamma_L b)$$

$$R_{13} = (n/b) J_n(\gamma_T b)$$

$$R_{14} = (n/b) Y_n(\gamma_T b)$$

$$R_{15} = -i\alpha\gamma_T J_n'(\gamma_T b)$$

$$R_{16} = -i\alpha\gamma_T Y_n'(\gamma_T b)$$

$$R_{21} = -(n/b) J_n(\gamma_L b)$$

$$R_{22} = -(n/b) Y_n(\gamma_L b)$$

$$R_{23} = -\gamma_T J_n'(\gamma_T b)$$

$$R_{24} = -\gamma_T Y_n'(\gamma_T b)$$

$$R_{25} = (i\alpha n/b) J_n(\gamma_T b)$$

$$R_{26} = (i\alpha n/b) Y_n(\gamma_T b)$$

$$R_{31} = i\alpha J_n(\gamma_L b)$$

$$R_{32} = i\alpha Y_n(\gamma_L b)$$

$$R_{33} = 0$$

$$R_{34} = 0$$

$$R_{35} = (\alpha^2 - k_T^2) J_n(\gamma_T b)$$

$$R_{36} = (\alpha^2 - k_T^2) Y_n(\gamma_T b)$$

Rows 4, 5, and 6 are obtained by setting b=a in rows 1, 2, and 3.

The Elastic Interior Matrices $[P^i(n,\alpha)]_{3\times3}$ and $[R^i(n,\alpha)]_{3\times3}$

$$P^i_{11} = 2\mu\gamma_L^2 J_n''(\gamma_L b) - \lambda k_L^2 J_n(\gamma_L b)$$
$$P^i_{12} = (2\mu n/b^2)[\gamma_T b J_n'(\gamma_T b) - J_n(\gamma_T b)]$$
$$P^i_{13} = -2i\alpha\mu\gamma_T^2 J_n''(\gamma_T b)$$
$$P^i_{21} = (2n\mu/b^2)[J_n(\gamma_L b) - \gamma_L b J_n'(\gamma_L b)]$$
$$P^i_{22} = (\mu/b^2)[2\gamma_T b J_n'(\gamma_T b) + (\gamma_T^2 b^2 - 2n^2) J_n(\gamma_T b)]$$
$$P^i_{23} = (2i\alpha\mu n/b^2)[b\gamma_T J_n'(\gamma_T b) - J_n(\gamma_T b)]$$
$$P^i_{31} = 2i\alpha\mu\gamma_L J_n'(\gamma_L b)$$
$$P^i_{32} = (i\alpha\mu n/b) J_n(\gamma_T b)$$
$$P^i_{33} = \mu\gamma_T(2\alpha^2 - k_T^2) J_n'(\gamma_T b)$$

$$R^i_{11} = \gamma_L J_n'(\gamma_L b)$$
$$R^i_{12} = (n/b) J_n(\gamma_T b)$$
$$R^i_{13} = -i\alpha\gamma_T J_n'(\gamma_T b)$$
$$R^i_{21} = -(n/b) J_n(\gamma_L b)$$
$$R^i_{22} = -\gamma_T J_n'(\gamma_T b)$$
$$R^i_{23} = (i\alpha n/b) J_n(\gamma_T b)$$
$$R^i_{31} = i\alpha J_n(\gamma_L b)$$
$$R^i_{32} = 0$$
$$R^i_{33} = (\alpha^2 - k_T^2) J_n(\gamma_T b)$$

The Elastic Exterior Matrices $[P^e(n,\alpha)]_{3*3}$ and $[R^e(n,\alpha)]_{3*3}$

$$P^e_{11} = 2\mu\gamma_L^2 H_n''(\gamma_L a) - \lambda k_L^2 H_n(\gamma_L a)$$
$$P^e_{12} = (2\mu n/a^2)[\gamma_T a H_n'(\gamma_T a) - H_n(\gamma_T a)]$$
$$P^e_{13} = -2i\alpha\mu\gamma_T^2 H_n''(\gamma_T a)$$
$$P^e_{21} = (2n\mu/a^2)[H_n(\gamma_L a) - \gamma_L a H_n'(\gamma_L a)]$$
$$P^e_{22} = (\mu/a^2)[2\gamma_T a H_n'(\gamma_T a) + (\gamma_T^2 a^2 - 2n^2) H_n(\gamma_T a)]$$
$$P^e_{23} = (2i\alpha\mu n/a^2)[a\gamma_T H_n'(\gamma_T a) - H_n(\gamma_T a)]$$
$$P^e_{31} = 2i\alpha\mu\gamma_L H_n'(\gamma_L a)$$
$$P^e_{32} = (i\alpha n\mu/a) H_n(\gamma_T a)$$
$$P^e_{33} = \mu\gamma_T(2\alpha^2 - k_T^2) H_n'(\gamma_T a)$$

$$R^e_{11} = \gamma_L H_n'(\gamma_L a)$$
$$R^e_{12} = (n/a) H_n(\gamma_T a)$$
$$R^e_{13} = -i\alpha\gamma_T H_n'(\gamma_T a)$$
$$R^e_{21} = -(n/a) H_n(\gamma_L a)$$
$$R^e_{22} = -\gamma_T H_n'(\gamma_T a)$$
$$R^e_{23} = (i\alpha n/a) H_n(\gamma_T a)$$
$$R^e_{31} = i\alpha H_n(\gamma_L a)$$
$$R^e_{32} = 0$$
$$R^e_{33} = (\alpha^2 - k_T^2) H_n(\gamma_T a)$$

APPENDIX B

The System Matrix [SM(n, α)] for a 2-layer Pipe
9*9

exterior matrix $[S^{e}(n,\alpha)]$
3*3

layer matrix $[S^{1}(n,\alpha)]$
6*6

layer matrix $[S^{2}(n,\alpha)]$
6*6

interior matrix $[S^{i}(n,\alpha)]$
3*3

$$
\begin{bmatrix}
S^1_{11}-S^e_{11} & S^1_{12}-S^e_{12} & S^1_{13}-S^e_{13} & S^1_{14} & S^1_{15} & S^1_{16} & 0 & 0 & 0 \\
S^1_{21}-S^e_{21} & S^1_{22}-S^e_{22} & S^1_{23}-S^e_{23} & S^1_{24} & S^1_{25} & S^1_{26} & 0 & 0 & 0 \\
S^1_{31}-S^e_{31} & S^1_{32}-S^e_{32} & S^1_{33}-S^e_{33} & S^1_{34} & S^1_{35} & S^1_{36} & 0 & 0 & 0 \\
-S^1_{41} & -S^1_{42} & -S^1_{43} & S^2_{11}-S^1_{44} & S^2_{12}-S^1_{45} & S^2_{13}-S^1_{46} & S^2_{14} & S^2_{15} & S^2_{16} \\
-S^1_{51} & -S^1_{52} & -S^1_{53} & S^2_{21}-S^1_{54} & S^2_{22}-S^1_{55} & S^2_{23}-S^1_{56} & S^2_{24} & S^2_{25} & S^2_{26} \\
-S^1_{61} & -S^1_{62} & -S^1_{63} & S^2_{31}-S^1_{64} & S^2_{32}-S^1_{65} & S^2_{33}-S^1_{66} & S^2_{34} & S^2_{35} & S^2_{36} \\
0 & 0 & 0 & -S^2_{41} & -S^2_{42} & -S^2_{43} & S^i_{11}-S^2_{44} & S^i_{12}-S^2_{45} & S^i_{13}-S^2_{46} \\
0 & 0 & 0 & -S^2_{51} & -S^2_{52} & -S^2_{53} & S^i_{21}-S^2_{54} & S^i_{22}-S^2_{55} & S^i_{23}-S^2_{56} \\
0 & 0 & 0 & -S^2_{61} & -S^2_{62} & -S^2_{63} & S^i_{31}-S^2_{64} & S^i_{32}-S^2_{65} & S^i_{33}-S^2_{66}
\end{bmatrix}
$$

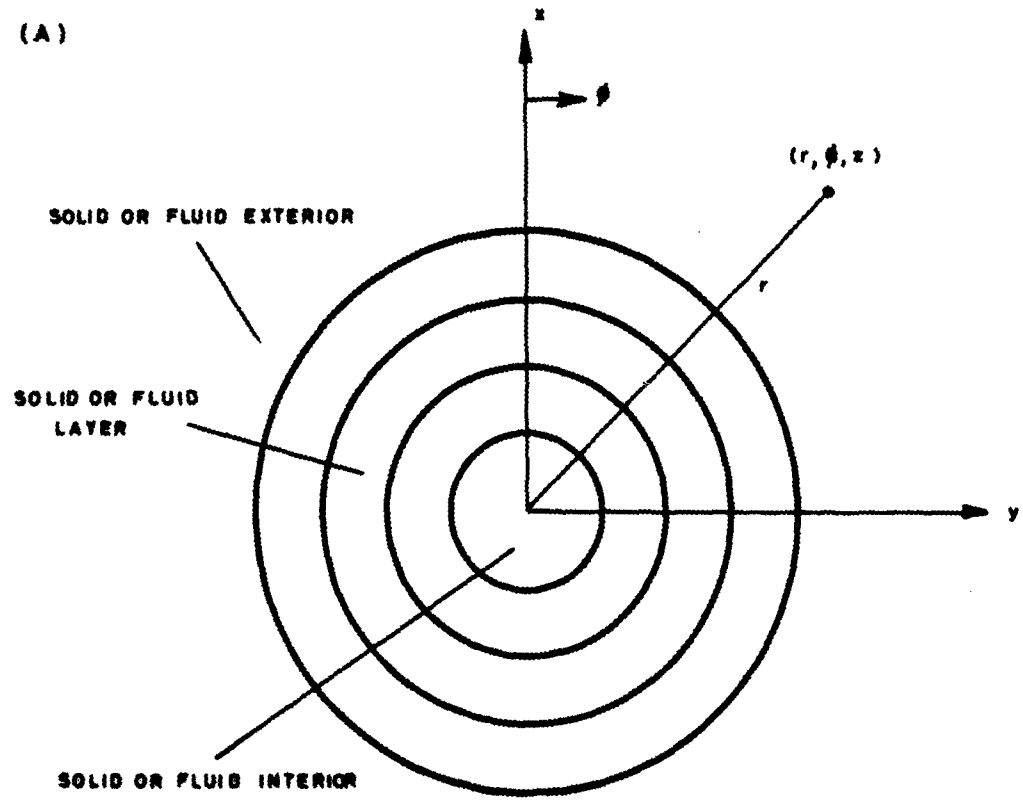

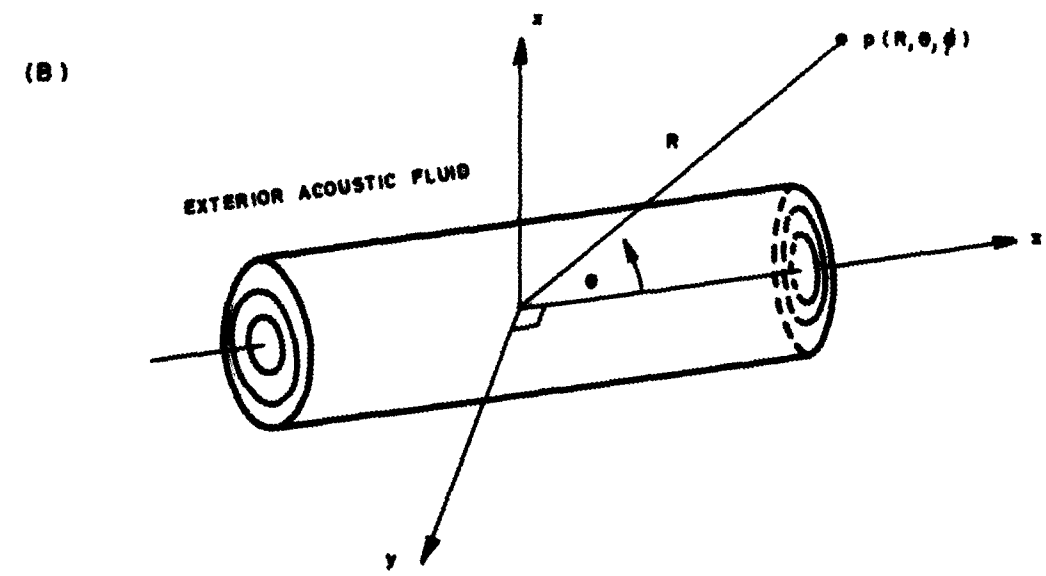

FIG. 1 (A) CROSS-SECTION THROUGH LAYERED SYSTEM
(B) GEOMETRY FOR FAR-FIELD ACOUSTIC RADIATION

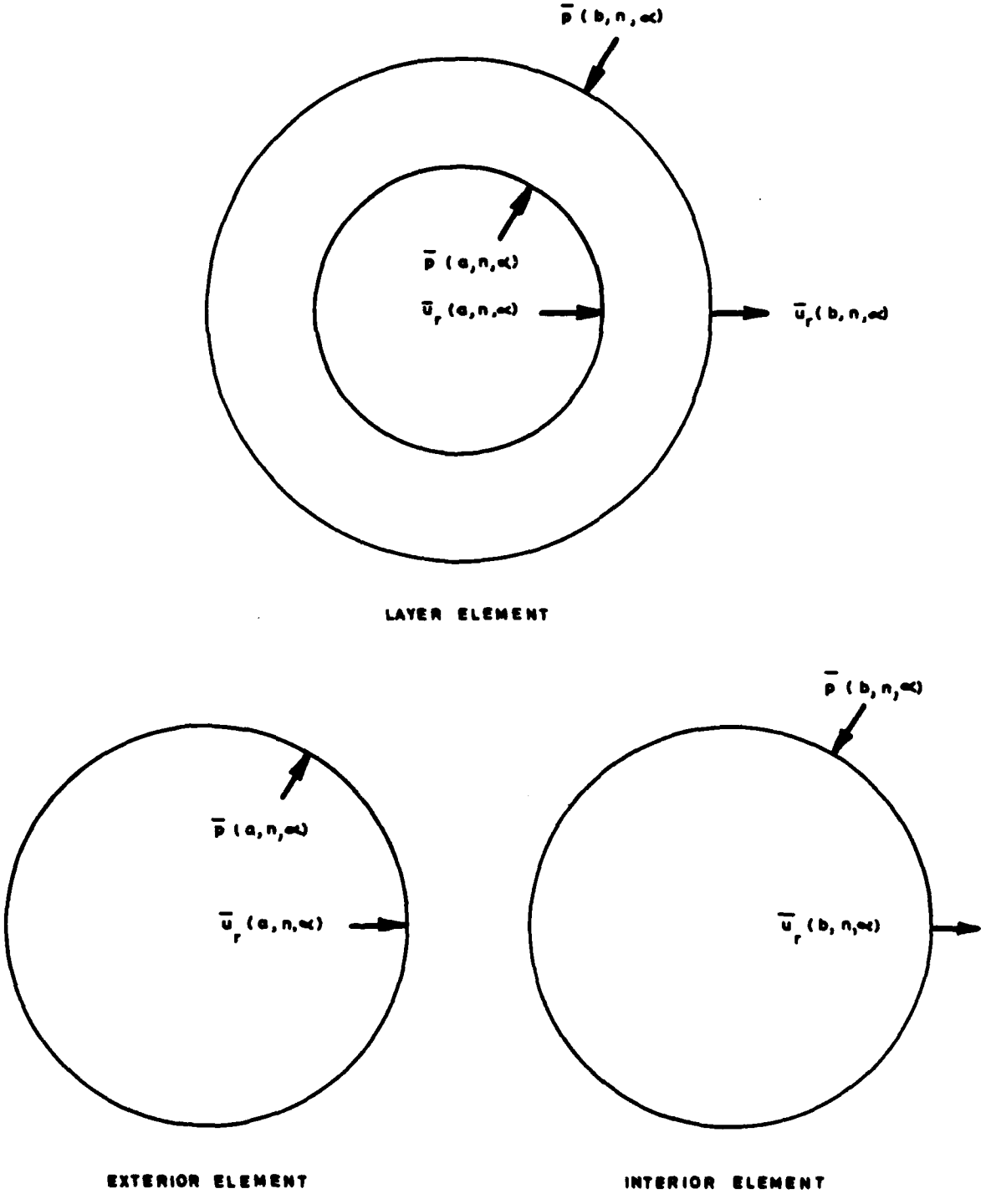

FIG. 2 SPECTRAL PRESSURES AND DISPLACEMENTS OF ACOUSTIC FLUID ELEMENTS

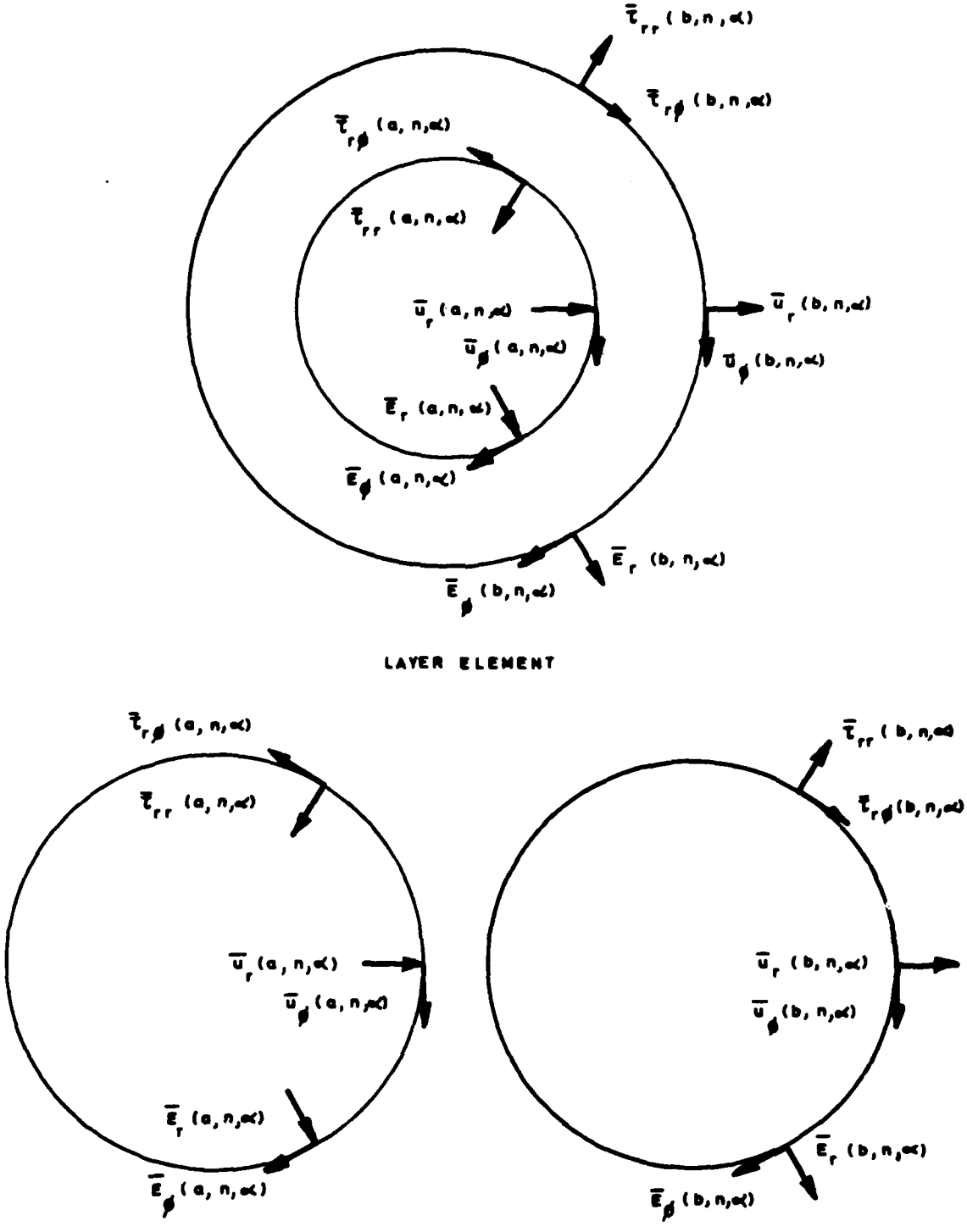

FIG. 3 SPECTRAL STRESSES AND DISPLACEMENTS OF ELASTIC SOLID OR VISCOUS FLUID ELEMENTS

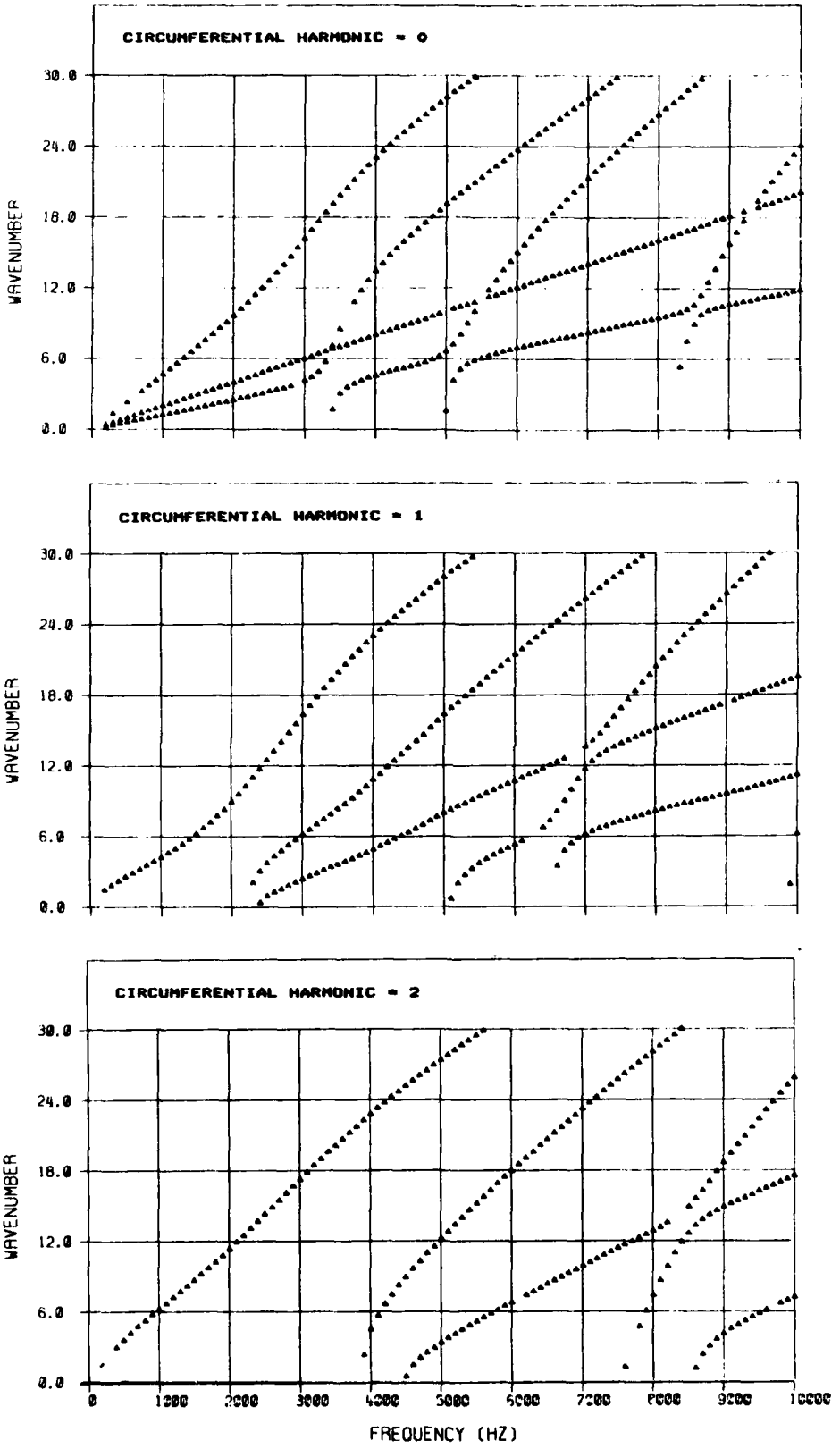

FIG. 4 AXIAL WAVENUMBER V. FREQUENCY PLOTS STEEL PIPE

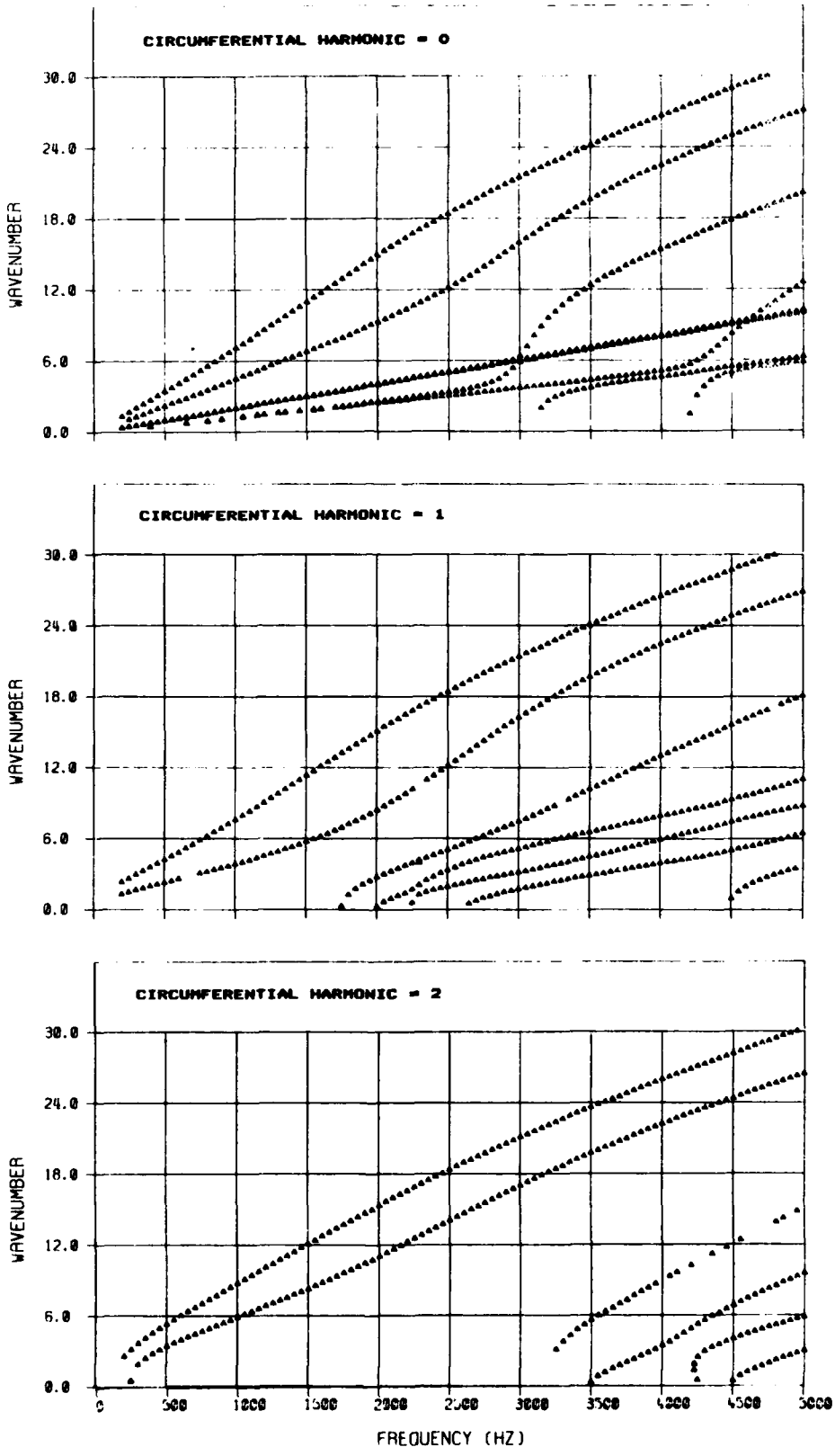

FIG. 5 AXIAL WAVENUMBER V. FREQUENCY PLOTS COMPOSITE PIPE (STEEL - WATER - STEEL)

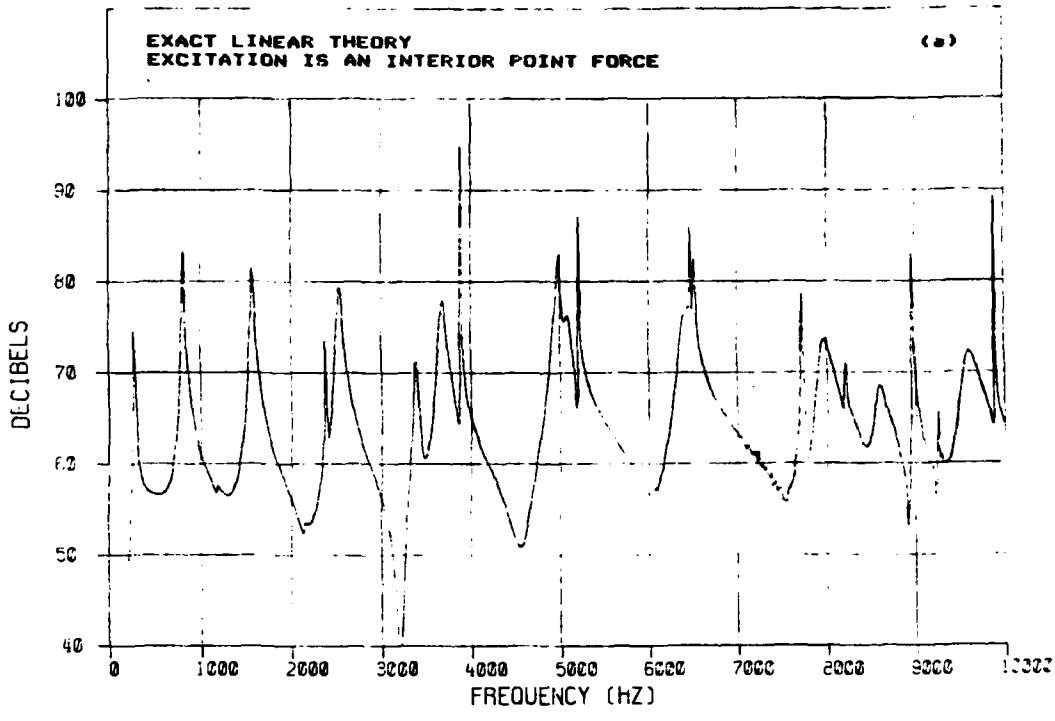

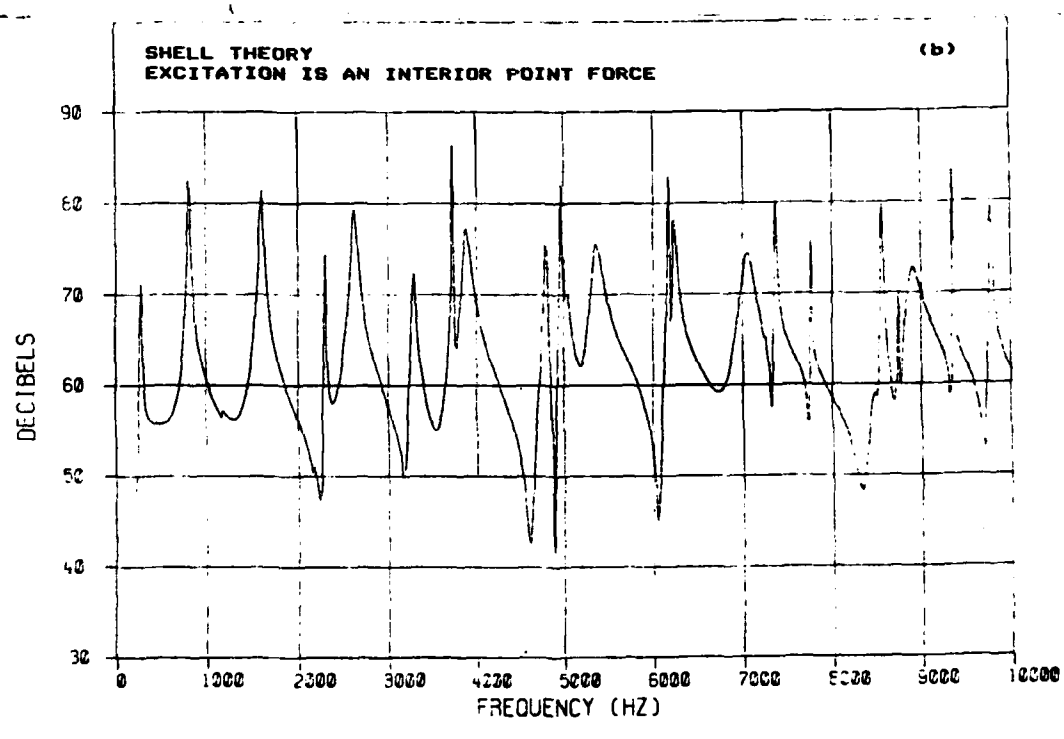

FIG. 6 COMPARISON OF EXACT LINEAR THEORY AND SHELL THEORY, θ=90°

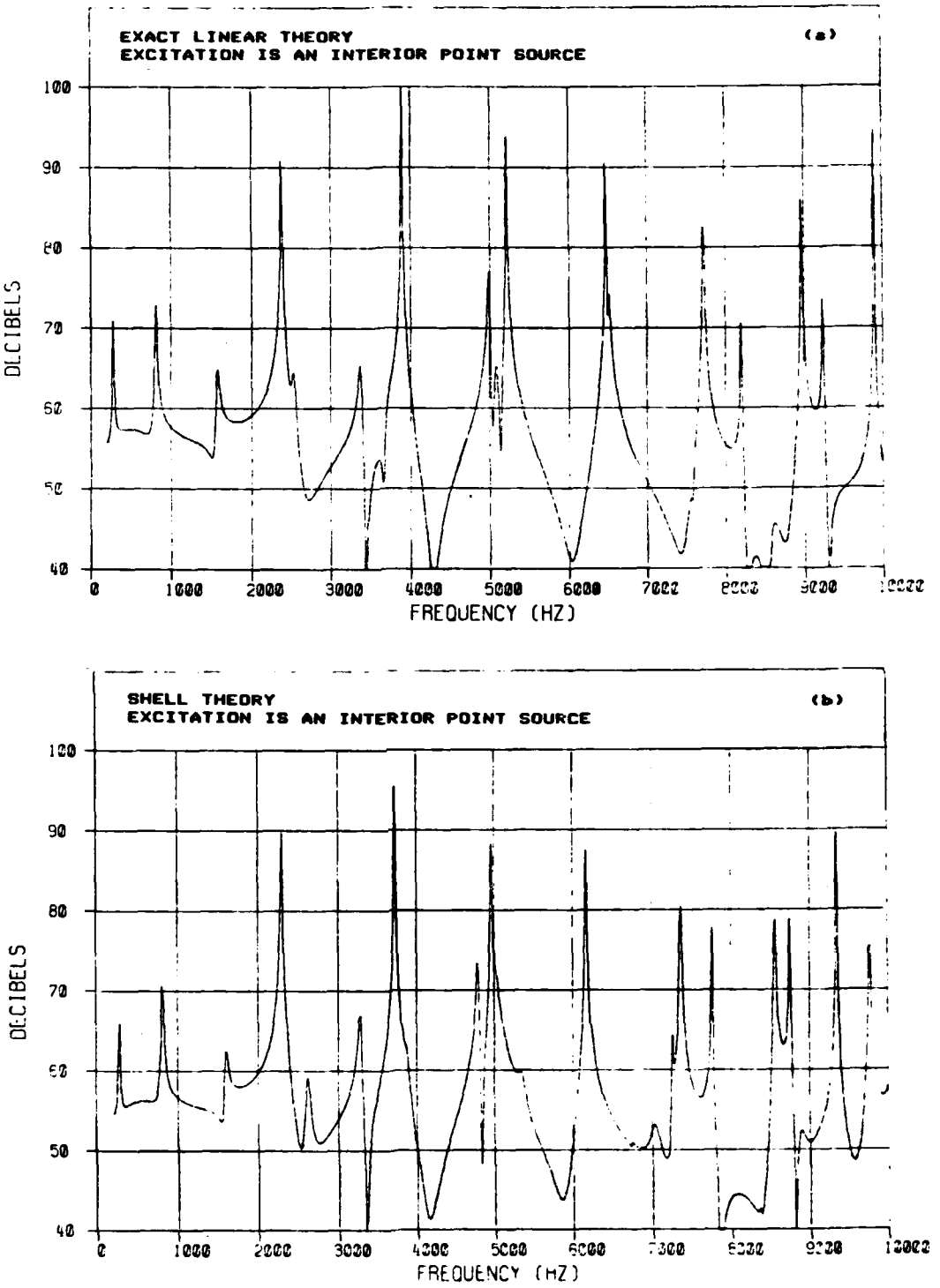

FIG. 7 COMPARISON OF EXACT LINEAR THEORY AND SHELL THEORY, $\theta=90°$

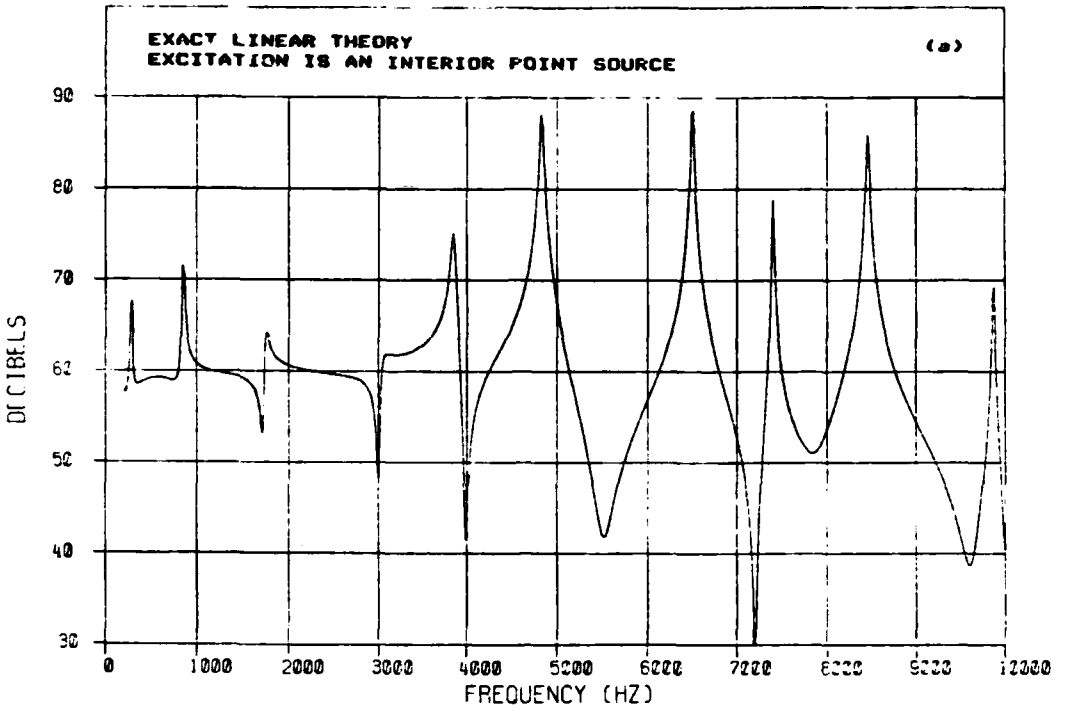

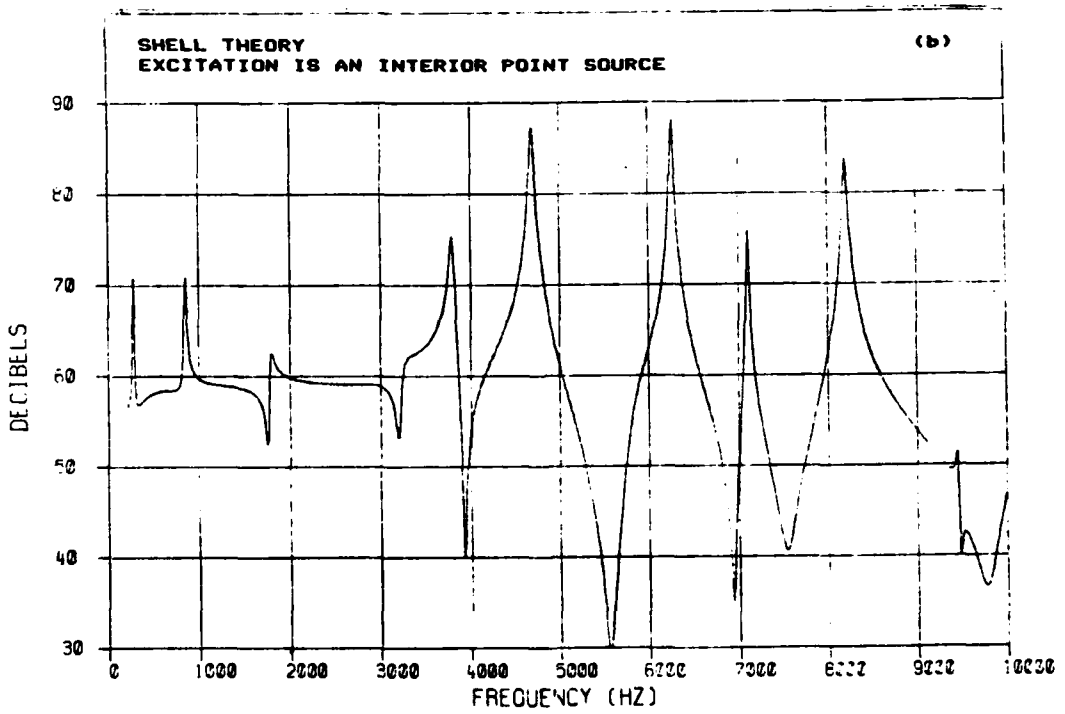

FIG. 8 COMPARISON OF EXACT LINEAR THEORY AND SHELL THEORY, $\theta = 80°$

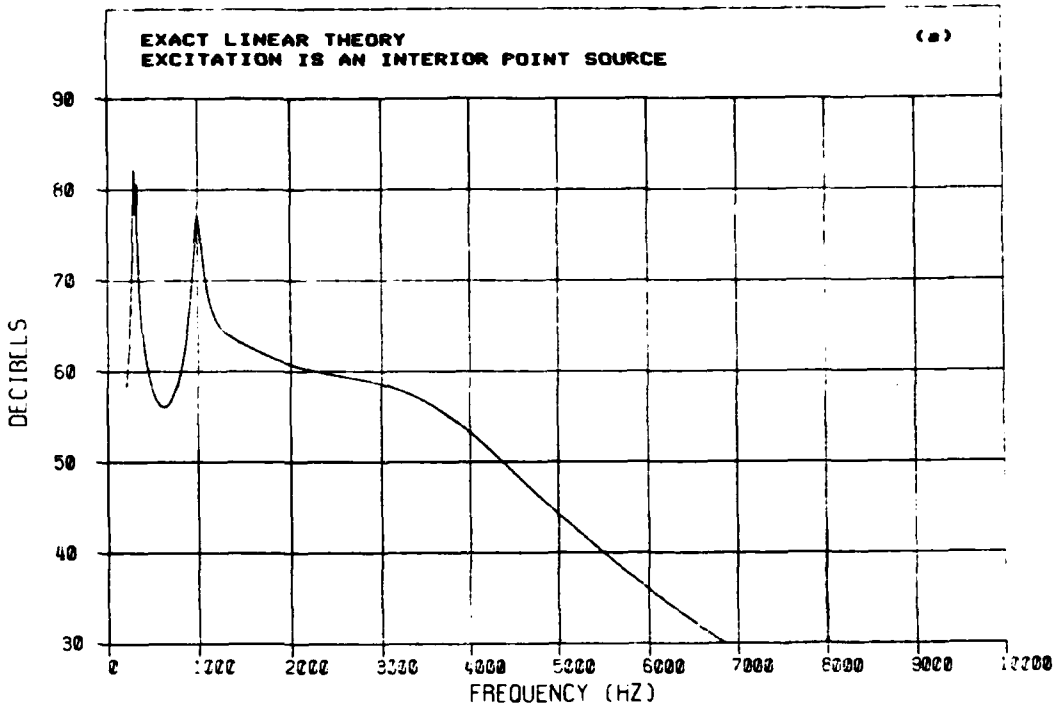

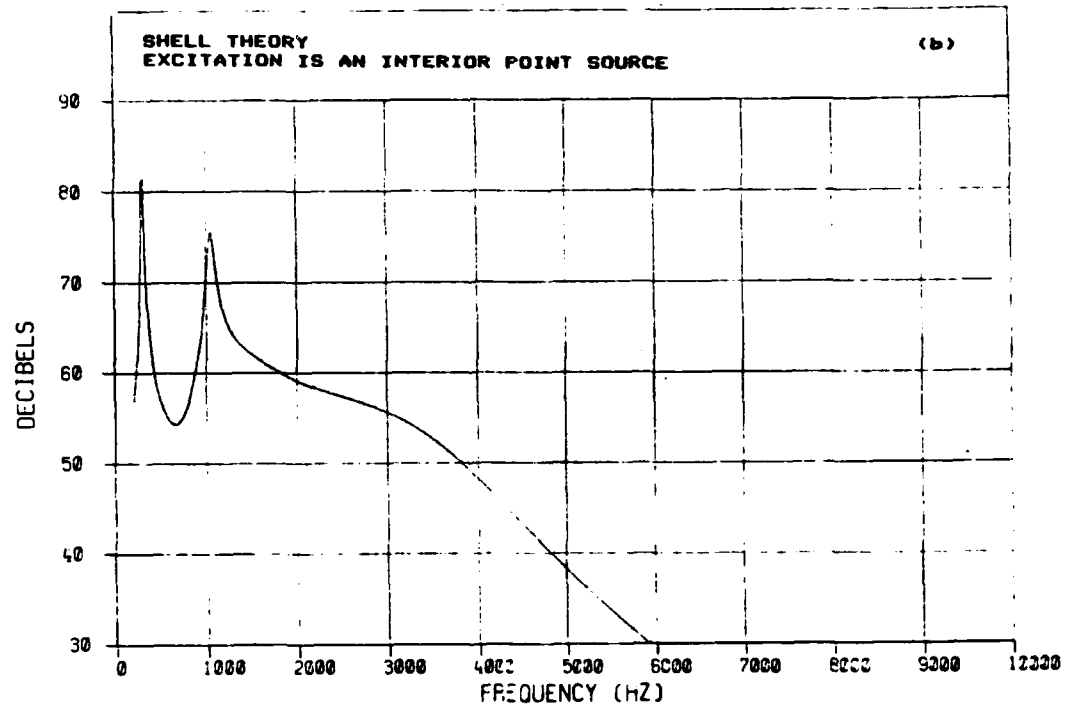

FIG. 9 COMPARISON OF EXACT LINEAR THEORY AND SHELL THEORY, $\theta = 70°$

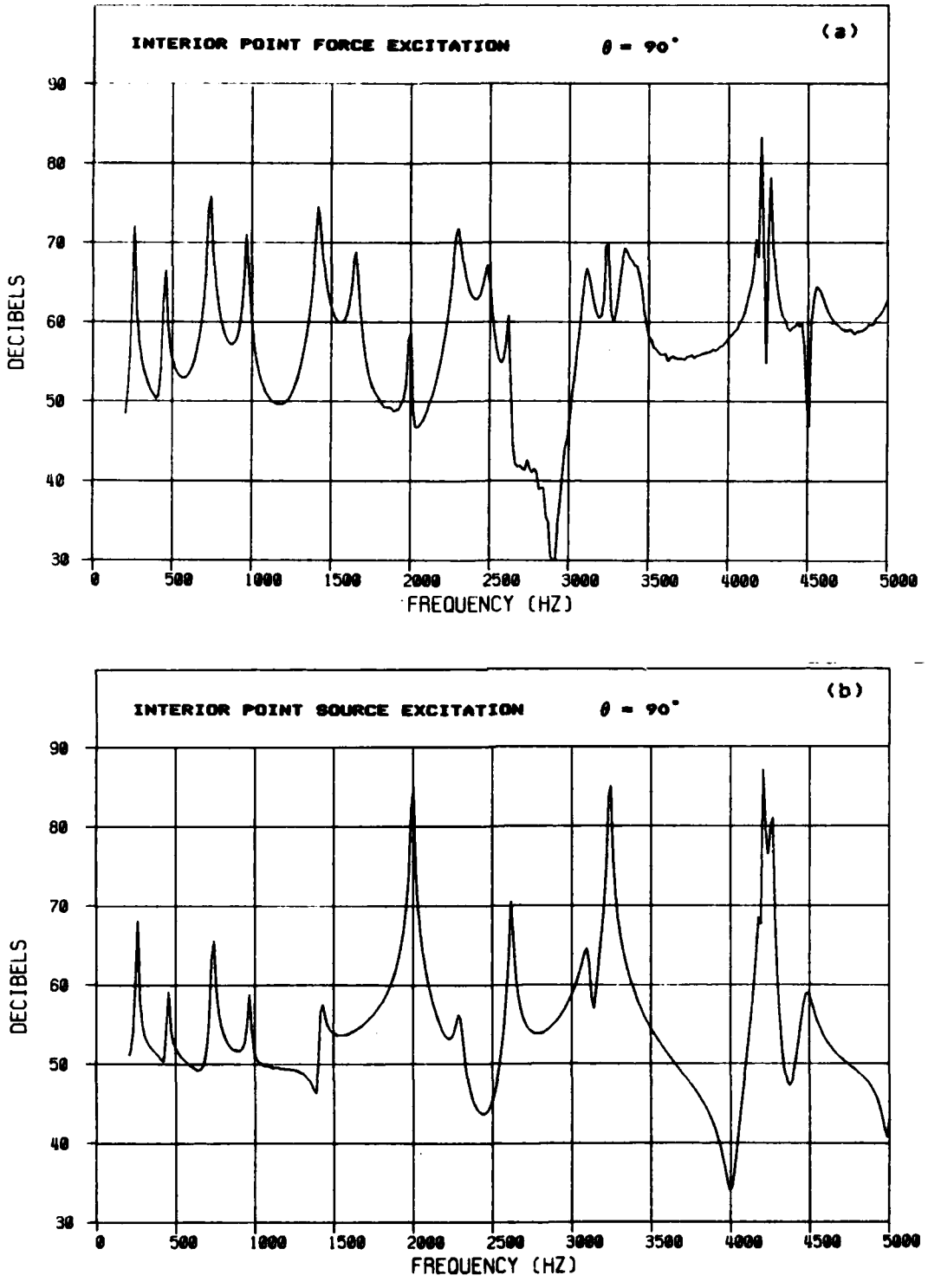

FIG. 10 RADIATION FROM COMPOSITE PIPE (STEEL - WATER - STEEL)

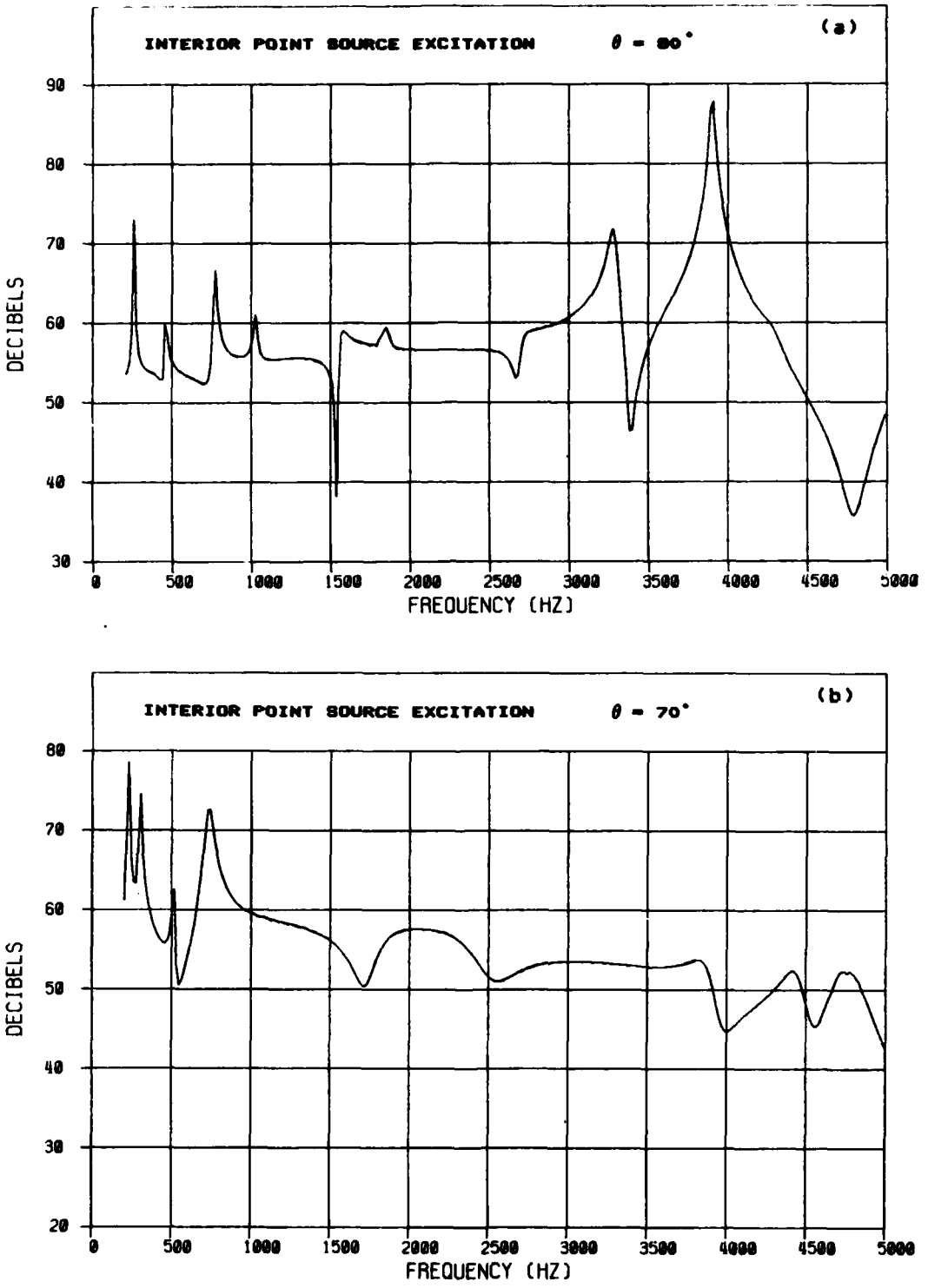

FIG. 11 RADIATION FROM COMPOSITE PIPE (STEEL - WATER - STEEL)

DISTRIBUTION

	Copy No
DGRA/CS(RN)/DNA	1
DAUWE (Dr I Roebuck)	2
DES Washington	3
CS(R) 2e (Navy)	4
DG Ships/DPT 17	5
DRIC	6-45
AMTE (Dunfermline)	46
AMTE (Teddington) File	47-54
AMTE (Mr J H James)	55
AMTE (Ms E A Skelton)	56
AMTE (Teddington) Division N1 File	57

END

DATE
FILMED

5 83

DTIC